Inorganic Chemistry

ARTICLE

pubs.acs.org/IC

Single Molecule Magnet Behavior of a Pentanuclear Mn-Based Metallacrown Complex: Solid State and Solution Magnetic Studies

Curtis M. Zaleski,[†] Simon Tricard,[‡] Ezra C. Depperman,[§] Wolfgang Wernsdorfer,[∥] Talal Mallah,[*,‡] Martin L. Kirk,[*,§] and Vincent L. Pecoraro[*,⊥]

[†]Department of Chemistry, Shippensburg University, Shippensburg, Pennsylvania 17257-2200, United States

[‡]Institut de Chimie Moléculaire et des Matériaux d'Orsay, CNRS, Université Paris Sud 11, 91405 Orsay Cedex, France

[§]Department of Chemistry, The University of New Mexico, Albuquerque, New Mexico 87131-0001, United States

[∥]Institut Néel, UPR CNRS 5051, BP 166, 25 Avenue des Martyrs, 38042 Grenoble Cedex 9 France

[⊥]Department of Chemistry, University of Michigan, 930 N. University Avenue, Ann Arbor, Michigan 48109-1055, United States

Supporting Information

ABSTRACT: The magnetic behavior of the pentanuclear complex of formula $Mn^{II}(O_2CCH_3)_2[12\text{-}MC_{Mn^{III}(N)shi}\text{-}4](DMF)_6$, **1**, was investigated using magnetization and magnetic susceptibility measurements both in the solid state and in solution. Complex **1** has a nearly planar structure, made of a central Mn^{II} ion surrounded by four peripheral Mn^{III} ions. Solid state variable-field dc magnetic susceptibility experiments demonstrate that **1** possesses a low value for the total spin in the ground state; fitting appropriate expressions to the data results in antiferromangetic coupling both between the peripheral Mn^{III} ions ($J = -6.3$ cm^{-1}) and between the central Mn^{II} ion and the Mn^{III} ones ($J' = -4.2$ cm^{-1}). In order to obtain a reasonable fit, a relatively large single ion magnetic anisotropy (D) value of 1 cm^{-1} was necessary for the central Mn^{II} ion. The single crystal magnetization measurements using a microsquid array display a very slight opening of the hysteresis loop but only at a very low temperature (0.04 K), which is in line with the ac susceptibility data where a slow relaxation of the magnetization occurs just around 2 K. In frozen solution, complex **1** displays a frequency dependent ac magnetic susceptibility signal with an energy barrier to magnetization reorientation (E) and relaxation time at an infinite temperature (τ_o) of 14.7 cm^{-1} and 1.4×10^{-7} s, respectively, demonstrating the single molecule magnetic behavior in solution.

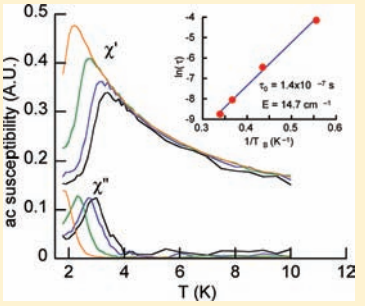

INTRODUCTION

During the past 20 years, molecular magnetism has been a very active field of research. In part, this is due to the discovery of new single molecule magnet (SMM) behavior in coordination compounds, where the perspective of storing information in a single magnetic nanosized object may become a reality.[1−15] Single molecule magnets are good candidates for these purposes because they display a magnetic hysteresis loop with a long relaxation time at zero dc magnetic field, even though this behavior, at the moment, is only observed at very low temperatures. This results from the presence of an anisotropy barrier for the reorientation of their magnetization. However, in order to use such SMMs for information storage, the hysteresis loop must be retained not only when the molecules are organized within the crystal but also when isolated. Very recently, reports on three different complexes have demonstrated that SMMs can maintain their magnetic bistability in isolation.[16−18] In the case of the Tb-double decker complex, a slight increase of the width of the hysteresis loop was observed, demonstrating the drawback of intermolecular interactions on the magnetic bistability of SMMs. Chemical stability is also required to study their magnetic behavior in solution and to utilize these isolated molecules in technological applications. Metallacrown-based complexes that contain lanthanide and transition metal ions have already been shown to behave as SMMs.[19−23] Furthermore, the architecture of these complexes[24−26] and the local symmetry of the metal ions has allowed for proper orientation of the axial distortion of the different metal ions in order to maximize the overall anisotropy.[27] The pentanuclear complex $Mn^{II}(O_2CCH_3)_2[12\text{-}MC_{Mn^{III}(N)shi}\text{-}4](DMF)_6$, **1**,[28] fulfills all of the above requirements: it has a disklike shape, the Jahn−Teller axial distortions of the four Mn^{III} ions are quasiparallel, and the

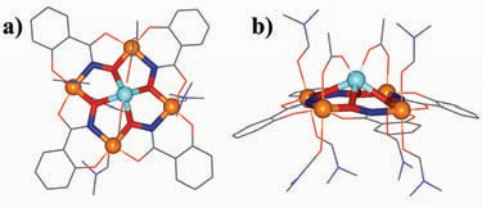

Figure 1. X-ray crystal structure of **1** along the pseudo-4 fold axis (a) and from the side (b). Color scheme: orange spheres, Mn^{III}; aqua sphere, Mn^{II}; red tube, oxygen; blue tube, nitrogen; gray line, carbon.

Received: April 26, 2011
Published: October 21, 2011

 © 2011 American Chemical Society

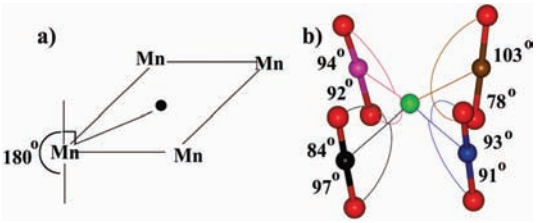

Figure 2. (a) Schematic diagram of a perfectly planar 12−MC−4 with the Jahn−Teller axes being collinear with respect to the estimated center of the Mn^{III}_4 plane ($O_{J\text{-}T}$−Mn^{III}−center). (b) Measured $O_{Jahn-Teller}$−Mn^{III}−center angles about the Mn^{III}_4 plane of **1** with only the Mn^{III} ions and the Jahn−Teller ligands shown for clarity. Color scheme: red sphere, oxygen; green sphere, estimated center; black sphere, Mn2; magenta sphere, Mn3; brown sphere, Mn4; blue sphere, Mn5.

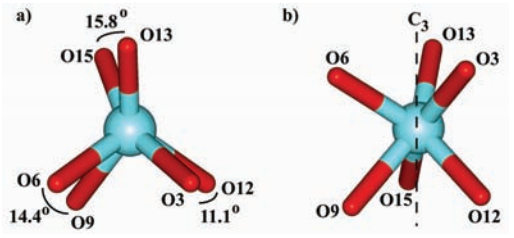

Figure 3. Coordination sphere about the central Mn^{II} ion of **1**. Note that the geometry is not octahedral but closer to trigonal prismatic.

Scheme 1. Coupling Scheme for 1

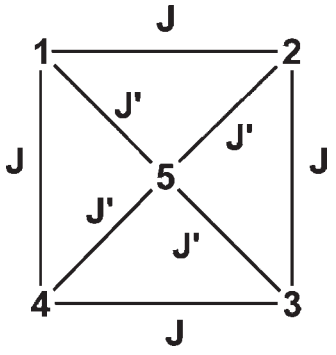

complex is stable in solution. In this paper, we report on the magnetic studies of **1** in the solid state and in solution.

RESULTS AND DISCUSSION

The structure of **1** is nearly planar (Figure 1) and orients all four peripheral Mn^{III} ions with their Jahn−Teller axes almost parallel, as depicted in Figure 2.[28] The geometry of the central Mn^{II} ion is closer to trigonal prismatic than octahedral with a principal symmetry axis close to C_3 (Figure 3).

Variable-temperature dc magnetic susceptibility experiments reveal that **1** is dominated by antiferromagnetic exchange interactions. The $\chi_M T$ product decreases upon cooling and reaches a value of 1.02 cm^3 K mol^{-1} at 2 K (Figure S1, Supporting Information). Fitting the linear $f(T) = 1/\chi_M$ data between 200 and 100 K leads to a Curie constant of 15.9 cm^3 K mol^{-1}, which

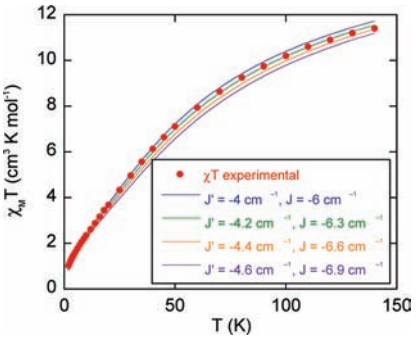

Figure 4. Analysis of the χT experimental data of **1** reveals that the four Mn^{III} ions of the ring are antiferromagnetically coupled ($J = -6.3$ cm^{-1}), and the central Mn^{II} ion is antiferromagnetically coupled to the ring Mn^{III} ions ($J' = -4.2$ cm^{-1}).

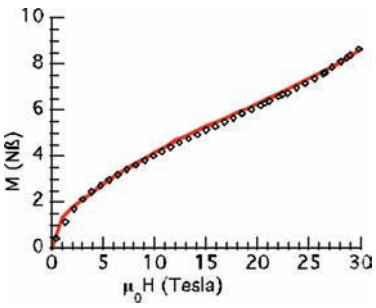

Figure 5. Variable-field dc magnetic susceptibility measurements of **1**. The red line indicates the best fit to the experimental data.

corresponds well to that of the isolated ions: four Mn^{III} ions ($S = 2$, $g_{Mn(III)} = 1.98$) and one Mn^{II} ion ($S = 5/2$, $g_{Mn(II)} = 2.0$; Figure S2, Supporting Information). In order to simulate the magnetic data, we assumed an interaction topology with two exchange coupling parameters: J (between two Mn^{III} ions) and J' (between the central Mn^{II} and the peripheral Mn^{III} ions; Scheme 1) using the following spin Hamiltonian: $H = -J(S_1 \cdot S_2 + S_2 \cdot S_3 + S_3 \cdot S_4 + S_4 \cdot S_1) - J' S_5 \cdot (S_1 + S_2 + S_3 + S_4)$.

The susceptibility and the magnetization data were calculated using the MAGPACK software.[29,30] The susceptibility was first calculated by neglecting the local anisotropy of the metal ions; the best results were obtained with a J'/J ratio of 2:3 ($J' = -4.2$ cm^{-1}; $J = -6.3$ cm^{-1}; Figure 4). The corresponding spin ladder reveals that the ground state is $S_T = 1/2$ and separated by only 2 cm^{-1} from the first $S_T = 3/2$ excited state. The next excited states are $S_T = 1/2$ and $S_T = 3/2$ that lie 6.6 cm^{-1} above the ground spin state.

The $f(\mu_0 H) = M$ magnetization data (0−30 T at 0.6 K) clearly indicates that anisotropy effects in low-lying S_T states and spin sublevel crossings are important in describing the magnetic behavior of **1** in applied magnetic fields. If this were not the case, well-defined steps would have been observed in the low temperature magnetization data. In order to take into account the effects of the uniaxial anisotropy on the magnetization of **1**, magnetization plots were constructed for different values of the local spin Hamiltonian parameters by constraining $D(Mn^{II})$ and $D(Mn^{III})$ as fixed parameters and using the J' and J values obtained from the initial analysis of the susceptibility data. These calculations were performed iteratively until a reasonable simulation was obtained with the following parameters: $J' = -4.2$ cm^{-1},

dx.doi.org/10.1021/ic2008792 |Inorg. Chem. 2011, 50, 11348–11352

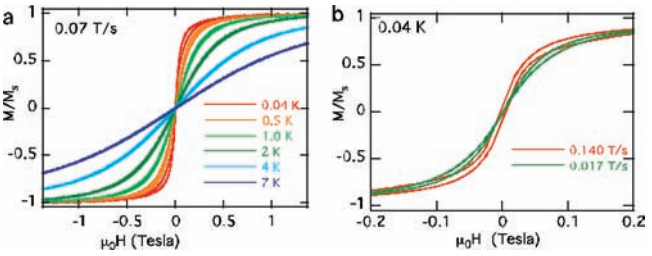

Figure 6. (a) Micro-SQUID magnetization of **1** versus the applied field ($\mu_o H$) at a sweep rate of 0.07 T/s at various temperatures and (b) at 0.04 K at various sweep rates. The width of the hysteresis loop increases with an increase in the sweep rate.

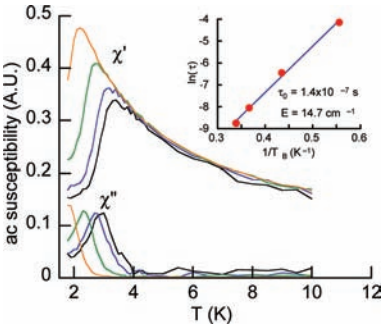

Figure 7. Variable temperature ac magnetic susceptibility measurements of **1** in DMF. The signal is frequency dependent, indicating SMM behavior. Color scheme: black, 1000 Hz; blue, 500 Hz; green, 100 Hz; orange, 10 Hz. Inset: Determination of the energy barrier for the relaxation of magnetization. The line is the least-squares best fit to the Arrhenius relationship.

$J = -6.0$ cm^{-1}, $D(\mathrm{Mn^{II}}) = +1$ cm^{-1}, $g(\mathrm{Mn^{II}}) = 2.0$ cm^{-1}, $D(\mathrm{Mn^{III}}) = -3.0$ cm^{-1}, and $g(\mathrm{Mn^{III}}) = 1.98$ (Figure 5). This simulation shows that the single ion anisotropy values and the exchange coupling parameters are on the same order of magnitude; therefore, the ground spin state cannot be expressed simply in terms of a total spin value. Additionally, the shape of the magnetization curve is very sensitive to small changes in these zero-field splitting parameters.

Although the magnitude of the D_{Si} value found for $\mathrm{Mn^{III}}$ is well within the range of other values reported in the literature,[31,32] the D_{Si} value determined for $\mathrm{Mn^{II}}$ is much larger than that anticipated for a single ion with a $^6A_1$ ground state. Typical D_{Si} values for octahedral $\mathrm{Mn^{II}}$ complexes are ca. 0.1−0.2 cm^{-1}, but such values lead to very poor fits to the reduced magnetization of **1**.[33] Interestingly, the local structure around $\mathrm{Mn^{II}}$ within the pentanuclear complex is rather unusual for a $\mathrm{Mn^{II}}$ ion. Typically, $\mathrm{Mn^{II}}$ ions adopt a coordination sphere that is only very slightly distorted from a regular octahedron leading to a given energy separation between the $^6A_1$ ground state term and the excited quadruplet and doublet terms ($^4T_1$ and $^2T_2$), which are responsible for the magnitude of the D_{Si}.[32] In contrast, the geometry around the $\mathrm{Mn^{II}}$ in **1** is markedly distorted from octahedral, with the MnO_6 unit possessing a pseudo C_3 axis (perpendicular to the face formed by the O6−O3−O13 atoms). In fact, the $\mathrm{Mn^{II}}$ geometry coordination is closer to trigonal prismatic than to octahedral (Figure 3) since the azimuthal angles (Φ) around the pseudo-C_3 axis range between 15.8 and 11.1° ($\Phi = 60°$ for an octahedron and 0° for a regular trigonal prism). This trigonal prismatic geometry leads to an increase in D_{Si}. Large D values for $\mathrm{Mn^{II}}$ have been observed in a low-symmetry (relative to octahedral) pentacoordinated complex.[34]

The dynamic magnetic behavior on a powder sample of **1** was probed by measuring the ac susceptibility at different frequencies of the oscillating magnetic field. A very weak frequency dependent in-phase (χ') signal was observed below 3 K. The χ' was associated with an out-of-phase (χ'') signal, which is also frequency dependent (Figure S3, Supporting Information). To investigate the magnetic behavior in the solid state at low temperature, a single crystal was oriented with the magnetic field parallel to its anisotropy axis on an array of micro-SQUIDs,[6] and the field was cycled between −1.4 and +1.4 T at different temperatures (0.04−7 K) and at several sweep rates. For a sweep rate of 0.07 T/s, a small opening of the hysteresis loop occurs below 1 K (Figure 6a), suggesting the occurrence of a slow relaxation of the magnetization for $\mu_0 H \neq 0$. In order to check whether this opening is due to a relaxation of the magnetization, the sweep rate was increased to 0.14 T/s. This resulted in an increase in the hysteresis loop at zero magnetic field at 0.04 K (Figure 6b). The dependence of the hysteresis loop width on the sweep rate is a signature of a slow magnetization relaxation and signals SMM behavior and not the onset of long-range magnetic order, which is independent of the magnetic field sweep rate. The closed loop at the slow sweep rate of 0.07 T/s is the result of a fast relaxation that is probably due to magnetization tunneling at zero field.

In order to eliminate solid state lattice effects on the properties of **1**, we have investigated the dynamic magnetization behavior of **1** in frozen DMF solution in zero applied dc magnetic field. The χ' and χ'' data display frequency-dependent maxima above 1.8 K (Figure 7), which was not the case in the solid state. The dependence of the maxima in χ'' with frequency is analyzed by plotting $\ln(\tau)$ as a function of $1/T_B$, where τ ($= 1/2\pi f$) is the relaxation time and T_B the temperature of the χ'' maximum for a given frequency. These data display Arrhenius type behavior with a relaxation time $\tau = \tau_0 \exp(E/kT_B)$. Here, E (14.7 cm^{-1}) is the energy barrier for the reorientation of the magnetization and τ_0 (1.4×10^{-7} s) is the relaxation time at infinite temperature. The Arrhenius type behavior of the magnetization relaxation and the rather large τ_0 value for **1** indicate that SMM behavior occurs above $T = 1.8$ K in solution, while in the solid state this behavior is observed only at lower temperatures.

The central $\mathrm{Mn^{II}}$ ion is extremely important to the observed SMM behavior of **1**. The analogous $Li\{Li(Cl)_2[12\text{-}MC_{Mn^{III}(N)shi}\text{-}4]\}$ complex, with Li^+ replacing the central $\mathrm{Mn^{II}}$, has a diamagnetic $S = 0$ ground state with $J = -4.0$ cm^{-1}, $J' = 0$ cm^{-1}, and $g = 1.9$ (Figure S4, Supporting Information).[35] Moreover, ac studies indicate that the Li^+ analogue exhibits no slow relaxation behavior (Figure S5, Supporting Information). This result is consistent with the stability of complex **1** in DMF since the loss of the $\mathrm{Mn^{II}}$ would have led to a diamagnetic complex and no SMM behavior.

The examination of the structure of **1** shows the absence of H bonds within the lattice, so only dipolar interactions may be present at low temperatures. The increase of the blocking temperature may thus be ascribed to much weaker intermolecular dipolar interactions when the molecules are isolated in frozen DMF. Indeed, a recent study, on the relationship between spin−lattice relaxation and quantum tunneling rate for the ErW_{10} polyoxometalate single molecule magnet,[36] demonstrated that a decrease of the dipolar interactions upon

dx.doi.org/10.1021/ic2008792 |Inorg. Chem. 2011, 50, 11348–11352

dilution of the molecules in a diamagnetic matrix leads to a decrease of the tunneling rate and thus to increase the blocking temperature.[37]

CONCLUSION

Complex **1** provides a strategy to synthesize new single-molecule magnets. Furthermore, the planar topology of the complex allows the individual D_{Si} of each Mn^{III} to combine constructively and create a non-negligible overall magnet anisotropy in the complex. The central Mn^{II} ion allows for a nonzero ground spin state that leads to the observed SMM behavior of the complex. However, it is not easy to discern the role of the central Mn^{II} ion with respect to its contribution to the overall ground state magnetoanisotropy, D_{ST}. The chemical flexibility of metallacrown complexes permits the preparation of new complexes with this same skeleton structure but possessing other magnetic central metal ions in place of Mn^{II}. Ni^{II} has a coordination chemistry similar to that of Mn^{II} and should be an excellent candidate for introducing additional single-ion anisotropy contributions to a large molecular magnetic anisotropy since hexacoordinate Ni^{II} can possess uniaxial anisotropies with D_{Si} values as large as -10 cm^{-1}.[38] Therefore, the strategy of central metal ion replacement could enhance the molecular anisotropy of the complex and result in even higher blocking temperatures. Furtheremore, the architecture of such metallacrown complexes induces a large stability in solution, allowing the occurrence of the SMM behavior as isolated molecules.

EXPERIMENTAL SECTION

The synthesis of **1** has been reported previously.[28] All dc magnetic susceptibility measurements were conducted on powered samples mulled in eicosane to prevent torquing of the sample in high applied dc magnetic fields. All samples were packed into gelatin capsules and placed in a drinking straw sample holder. All magnetic susceptibility values were corrected with Pascal's constants, and corrections were applied for the sample holder. Isofield variable-temperature dc magnetic susceptibility measurements were performed at 0.25 T on a Quantum Design MPMS SQUID from 2 to 300 K. Isothermal variable field dc magnetization measurements were performed using a vibrating sample magnetometer (VSM) operating at 0.6 K in an applied magnetic field of 0−30 T. All variable-temperature ac magnetic susceptibility measurements were performed on an MPMS SQUID magnetometer between 2 and 10 K in zero applied dc magnetic field with a 3.5 G ac alternating drive magnetic field operating at frequencies between 10 and 1000 Hz. The ac studies were conducted on the powdered sample mulled in eicosane and on the frozen DMF solution.

ASSOCIATED CONTENT

Supporting Information. Suceptibility data for complexes **1** and $Li\{Li(Cl)_2[12\text{-}MC_{Mn^{III}(N)shi}\text{-}4]\}$ are available as Supporting Information. This material is available free of charge via the Internet at http://pubs.acs.org.

AUTHOR INFORMATION

Corresponding Author

*E-mail: mlkirk@unm.edu, talal.mallah@u-psud.fr, vlpec@umich.edu.

ACKNOWLEDGMENT

V.L.P. thanks the National Science Foundation for financial support (CHE-0111428) and Mr. Ted Boron for useful discussions. M.L.K. thanks the National Science Foundation for financial support (CHE-1012928). We thank the National High Magnetic Field Laboratory at Florida State University, Reza Lolee (Physics and Astronomy Department, Michigan State University), and Prof. Meigan Aronson (Physics Department, University of Michigan) for use of their facilities.

REFERENCES

(1) Caneschi, A.; Gatteschi, D.; Sessoli, R.; Barra, A. L.; Brunel, L. C.; Guillot, M. *J. Am. Chem. Soc.* **1991**, *113*, 5873–5874.
(2) Sessoli, R.; Gatteschi, D.; Caneschi, A.; Novak, M. A. *Nature* **1993**, *365*, 141–143.
(3) Sessoli, R.; Tsai, H. L.; Schake, A. R.; Wang, S. Y.; Vincent, J. B.; Folting, K.; Gatteschi, D.; Christou, G.; Hendrickson, D. N. *J. Am. Chem. Soc.* **1993**, *115*, 1804–1816.
(4) Sun, Z. M.; Grant, C. M.; Castro, S. L.; Hendrickson, D. N.; Christou, G. *Chem. Commun.* **1998**, 721–722.
(5) Christou, G.; Gatteschi, D.; Hendrickson, D. N.; Sessoli, R. *MRS Bull.* **2000**, *25*, 66–71.
(6) Wernsdorfer, W. *Adv. Chem. Phys.* **2001**, *118*, 99–190.
(7) Sokol, J. J.; Hee, A. G.; Long, J. R. *J. Am. Chem. Soc.* **2002**, *124*, 7656–7657.
(8) Gatteschi, D.; Sessoli, R. *Angew. Chem., Int. Ed.* **2003**, *42*, 268–297.
(9) Ishikawa, N.; Sugita, M.; Ishikawa, T.; Koshihara, S.; Kaizu, Y. *J. Am. Chem. Soc.* **2003**, *125*, 8694–8695.
(10) Milios, C. J.; Vinslava, A.; Wernsdorfer, W.; Moggach, S.; Parsons, S.; Perlepes, S. P.; Christou, G.; Brechin, E. K. *J. Am. Chem. Soc.* **2007**, *129*, 2754–+.
(11) Berlinguette, C. P.; Vaughn, D.; Canada-Vilalta, C.; Galan-Mascaros, J. R.; Dunbar, K. R. *Angew. Chem., Int. Ed.* **2003**, *42*, 1523–1526.
(12) Moragues-Canovas, M.; Riviere, P.; Ricard, L.; Paulsen, C.; Wernsdorfer, W.; Rajaraman, G.; Brechin, E. K.; Mallah, T. *Adv. Mater.* **2004**, *16*, 1101.
(13) Beltran, L. M. C.; Long, J. R. *Acc. Chem. Res.* **2005**, *38*, 325–334.
(14) Maheswaran, S.; Chastanet, G.; Teat, S. J.; Mallah, T.; Sessoli, R.; Wernsdorfer, W.; Winpenny, R. E. P. *Angew. Chem., Int. Ed.* **2005**, *44*, 5044–5048.
(15) Rebilly, J. N.; Mallah, T. *Struct. Bonding (Berlin)* **2006**, *122*, 103–131.
(16) Giusti, A.; Charron, G.; Mazerat, S.; Compain, J. D.; Mialane, P.; Dolbecq, A.; Riviere, E.; Wernsdorfer, W.; Bibouni, R. N.; Keita, B.; Nadjo, L.; Filoramo, A.; Bourgoin, J. P.; Mallah, T. *Angew. Chem., Int. Ed.* **2009**, *48*, 4949–4952.
(17) Kyatskaya, S.; Galan-Mascaros, J. R.; Bogani, L.; Hennrich, F.; Kappes, M.; Wernsdorfer, W.; Ruben, M. *J. Am. Chem. Soc.* **2009**, *131*, 15143–15151.
(18) Mannini, M.; Pineider, F.; Sainctavit, P.; Danieli, C.; Otero, E.; Sciancalepore, C.; Talarico, A. M.; Arrio, M. A.; Cornia, A.; Gatteschi, D.; Sessoli, R. *Nat. Mater.* **2009**, *8*, 194–197.
(19) Dendrinou-Samara, C.; Alexiou, M.; Zaleski, C. M.; Kampf, J. W.; Kirk, M. L.; Kessissoglou, D. P.; Pecoraro, V. L. *Angew. Chem., Int. Ed.* **2003**, *42*, 3763–3766.
(20) Zaleski, C. M.; Depperman, E. C.; Kampf, J. W.; Kirk, M. L.; Pecoraro, V. L. *Angew. Chem., Int. Ed.* **2004**, *43*, 3912–3914.
(21) Zaleski, C. M.; Depperman, E. C.; Dendrinou-Samara, C.; Alexiou, M.; Kampf, J. W.; Kessissoglou, D. P.; Kirk, M. L.; Pecoraro, V. L. *J. Am. Chem. Soc.* **2005**, *127*, 12862–12872.
(22) Zaleski, C. M.; Depperman, E. C.; Kampf, J. W.; Kirk, M. L.; Pecoraro, V. L. *Inorg. Chem.* **2006**, *45*, 10022–10024.
(23) Zaleski, C. M.; Kampf, J. W.; Mallah, T.; Kirk, M. L.; Pecoraro, V. L. *Inorg. Chem.* **2007**, *46*, 1954–1956.

(24) Pecoraro, V. L.; Stemmler, A. J.; Gibney, B. R.; Bodwin, J. J.; Wang, H.; Kampf, J. W.; Barwinski, A. *Prog. Inorg. Chem.* **1997**, *45*, 83–177.
(25) Stemmler, A. J.; Kampf, J. W.; Pecoraro, V. L. *Angew. Chem., Int. Ed.* **1996**, *35*, 2841–2843.
(26) Mezei, G.; Zaleski, C. M.; Pecoraro, V. L. *Chem. Rev.* **2007**, *107*, 4933–5003.
(27) Boron, T.; Kampf, J. W.; Pecoraro, V. L. *Inorg. Chem.* **2010**, *49*, 9104–9106.
(28) Lah, M. S.; Pecoraro, V. L. *J. Am. Chem. Soc.* **1989**, *111*, 7258–7259.
(29) Borras-Almenar, J. J.; Coronado, E.; Ostrovsky, S. M.; Palii, A. V.; Tsukerblat, B. S. *Chem. Phys.* **1999**, *240*, 149–161.
(30) Borras-Almenar, J. J.; Clemente-Juan, J. M.; Coronado, E.; Tsukerblat, B. S. *J. Comput. Chem.* **2001**, *22*, 985–991.
(31) Bonadies, J. A.; Kirk, M. L.; Lah, M. S.; Kessissoglou, D. P.; Hatfield, W. E.; Pecoraro, V. L. *Inorg. Chem.* **1989**, *28*, 2037–2044.
(32) Barra, A. L.; Gatteschi, D.; Sessoli, R.; Abbati, G. L.; Cornia, A.; Fabretti, A. C.; Uytterhoeven, M. G. *Angew. Chem., Int. Ed. Engl.* **1997**, *36*, 2329–2331.
(33) Krzystek, J.; Ozarowski, A.; Telser, J. *Coord. Chem. Rev.* **2006**, *250*, 2308–2324.
(34) Pichon, C.; Mialane, P.; Riviere, E.; Blain, G.; Dolbecq, A.; Marrot, J.; Secheresse, F.; Duboc, C. *Inorg. Chem.* **2007**, *46*, 7710–7712.
(35) Gibney, B. R.; Wang, H.; Kampf, J. W.; Pecoraro, V. L. *Inorg. Chem.* **1996**, *35*, 6184–6193.
(36) AlDamen, M. A.; Clemente-Juan, J. M.; Coronado, E.; Marti-Gastaldo, C.; Gaita-Arino, A. *J. Am. Chem. Soc.* **2008**, *130*, 8874–8875.
(37) Luis, F.; Martinez-Perez, M. J.; O., M.; Coronado, E.; Cardona-Serra, S.; Marti-Gastaldo, C.; Clemente-Juan, J. M.; Sesé, J.; Drung, D.; Schurig, T. *Phys. Rev. B* **2010**, *82*, 060403–1−060403−4.
(38) Rogez, G.; Rebilly, J. N.; Barra, A. L.; Sorace, L.; Blondin, G.; Kirchner, N.; Duran, M.; van Slageren, J.; Parsons, S.; Ricard, L.; Marvilliers, A.; Mallah, T. *Angew. Chem., Int. Ed.* **2005**, *44*, 1876–1879.
(39) Koumousi, E. S.; Mukherjee, S.; Beavers, C. M.; Teat, S. J.; Christou, G.; Stamatatos, T. C. *Chem. Commun.* **2011**, *47*, 11128–11130.
(40) Meelich, K.; Zaleski, C. M.; Pecoraro, V. L. *Phil. Trans. Royal Soc.* **2008**, *363*, 1271–1281.

■ NOTE ADDED IN PROOF

An article appeared[39] after acceptance of this manuscript which contained a diamagnetic Ca(II) to form a $CaMn_4$ species[40] instead of the Li(I) metallacrown discussed in this report. These authors used the same coupling scheme reported here for $LiMn_4$ obtaining similar values for the J couplings of the metallacrown ring Mn(III) ions as we report herein and elsewhere.[26]